

Neutron scattering study of the effect of a random field on the three-dimensional dilute Ising antiferromagnet $\text{Fe}_{0.6}\text{Zn}_{0.4}\text{F}_2$

H. Yoshizawa,* R. A. Cowley,[†] and G. Shirane
Brookhaven National Laboratory, Upton, New York 11973

R. Birgeneau

Department of Physics, Massachusetts Institute of Technology, Cambridge, Massachusetts 02139

(Received 29 August 1984)

We report a comprehensive neutron scattering study of random-field effects in the three-dimensional Ising antiferromagnet $\text{Fe}_{0.6}\text{Zn}_{0.4}\text{F}_2$. The sample is the same one used in high-precision birefringence studies. The scattering is dependent on the prior history of the sample at all temperatures below a well-defined temperature which agrees with the phase boundary reported in the birefringence studies to within 0.2 K. When the sample is cooled in a field (FC), long-range order is not established and the scattering has a Lorentzian-squared profile with a width $K \approx H^2$, as found in the three-dimensional samples studied earlier with neutron scattering techniques. On the other hand, when the sample is cooled in zero field into the Néel state, the field raised and the temperature then increased (ZFC), the scattering close to the phase boundary consists of an antiferromagnetic Bragg component superimposed on scattering which is characteristic of the FC procedure. The Bragg component is absent when the crystal is heated above the phase boundary. In addition, if after field cooling the system is heated, the width of the scattering is unchanged until the phase boundary is reached. None of the existing $d_l=2$ low-temperature theories explains such behavior in the vicinity of the phase boundary. Above the phase boundary ZFC and FC results agree, indicating that the system is always in equilibrium. We have studied the critical behavior in this region and the scattering is very different from that with $H=0$. Specifically, the scattering profiles show a large Lorentzian-squared component and over a limited temperature range the inverse correlation length varies linearly with temperature.

I. INTRODUCTION

Since the pioneering theoretical work of Imry and Ma,¹ it has been recognized that random fields should have quite drastic effects both on the critical behavior and on the low-temperature states of systems undergoing phase transitions. Although random fields are ubiquitous in nature, until recently it seemed quite difficult to carry out systematic experiments on the random-field problem. However, Fishman and Aharony² pointed out that if a uniform magnetic field is applied to a random Ising antiferromagnet, then random staggered magnetic fields would be generated. They further suggested that this system would be isomorphous to the idealized problem of an Ising ferromagnet in a random field.

The Fishman-Aharony suggestion has stimulated a large number of experiments.³⁻¹⁰ It has resulted that the most accurate experiments could be performed on diluted transition-metal fluorides.⁴⁻⁹ For these systems high-quality single-crystal alloys may be grown in which the transition-metal ions are distributed at random with concentration gradients as small as 0.07%/mm. Further, the magnetic ions in transition-metal fluorides such as FeFe_2 are typically described by simple spin Hamiltonians with predominantly nearest-neighbor interactions. Particularly detailed information has been given by neutron scattering and birefringence techniques. We review very briefly the salient features of these experiments.

The neutron scattering experiments on the $d=2$ sys-

tem, $\text{Rb}_2\text{Co}_x\text{Mg}_{1-x}\text{F}_4$, and on the $d=3$ systems, $\text{Mn}_x\text{Zn}_{1-x}\text{F}_2$, $\text{Co}_x\text{Zn}_{1-x}\text{F}_2$ and $\text{Fe}_x\text{Zn}_{1-x}\text{F}_2$, have shown that when the crystal is cooled in a field long-range magnetic order is not achieved, and that at low temperatures the scattering profile as a function of wave vector has a Lorentzian-squared form. The width of the Lorentzian-squared form varies roughly as the square of the applied field. In all of the neutron measurements it was further found that at low temperatures the results were dependent on the prior history of the sample, and that these history-dependent effects persisted up to temperatures close to T_N . History-dependent effects have also been observed using thermal expansion measurements for $\text{Mn}_x\text{Zn}_{1-x}\text{Fe}_2$ (Ref. 4) and neutron scattering from $\text{Fe}_x\text{Mg}_{1-x}\text{Cl}_2$.¹⁰

Birefringence measurements on the $d=2$ system, $\text{Rb}_2\text{Co}_{1-x}\text{Mg}_{1-x}\text{F}_4$, showed that the sharp phase transition in zero field was rounded when cooled in an applied field. In the $d=3$ systems, $\text{Mn}_x\text{Zn}_{1-x}\text{F}_2$ and $\text{Fe}_x\text{Zn}_{1-x}\text{F}_2$, however, the peak in the temperature dependence of the birefringence, which is proportional to specific heat, was sharper in a field than with $H=0$, and consistent with $\alpha=0$ and concomitantly, an amplitude ratio $A/A'=1.0$. The shift in the transition temperature with field $T_N(H)$ was well described by the Fishman-Aharony scaling relations with $\phi=1.40 \pm 0.05$ in agreement with the random-exchange susceptibility exponent¹¹ γ , as predicted by theory. These results led to the first suggestion that $d=3$ systems in a random field exhibited $d=2$ critical phenomena, correspondingly it was concluded that

the lower critical dimension d_l was given by $2 \leq d_l < 3$.

In order to understand the relationship between the seemingly conflicting neutron scattering results and birefringence results, we have undertaken a study of the neutron scattering from the $\text{Fe}_{0.6}\text{Zn}_{0.4}\text{F}_2$ sample previously studied with birefringence techniques. We have made a particularly careful study of the history dependence of the scattering in the history dependence of the scattering in the neighborhood of $T_N(H)$ as we believe it is especially important to understand this aspect of the problem in more detail. We also report measurements of the critical scattering above $T_N(H)$. Some of the results have also been reported and analyzed in detail by Belanger *et al.*¹²

The format of this paper is as follows. Experimental procedures are described in Sec. II. The low-temperature results in the field-cooled configuration are given in Sec. III. In Sec. IV we describe experiments on the location of the phase boundary and hysteretic effects in the vicinity of $T_N(H)$. The behavior above $T_N(H)$ is presented in Sec. V. Discussion of the results, and conclusions in the contrast of recent theories¹³⁻¹⁹ are given in Sec. VI.

II. EXPERIMENTAL DETAILS

The sample, $\text{Fe}_{0.6}\text{Zn}_{0.4}\text{F}_2$, has the approximate dimensions $4 \times 4 \times 6 \text{ mm}^3$, with the larger dimension corresponding to the unique crystalline axis (c axis), the growth axis, and the concentration gradient. As discussed above, this single crystal is the same sample used in the recent birefringence measurements.⁸ Not only does this facilitate comparison between the two experiments, but this particular sample is of excellent quality, with a concentration gradient of only 0.07%/mm. Two separate experimental arrangements were used to collect data. In the first set of experiments, the sample was mounted on an aluminum holder with nearly the whole sample exposed. The platinum thermometer and control heater were situated about 25 cm from the sample, outside the magnet coils to reduce the field effect on the temperature reading. In the second set of experiments which were performed by Belanger and Yoshizawa,²⁰ the effect of the concentration gradient was minimized by masking with cadmium so that only about 1.5 mm along the c axis was exposed. A carbon-glass thermometer, which has only a slight field dependence, was placed in a copper block on which the sample was mounted and a separate control heater was wound around the block. With this improved configuration the temperature stability was better than 30 mK over the course of a scan. The neutron scattering was performed with a two-axis spectrometer at the Brookhaven National Laboratory high-flux beam reactor. The sample was oriented with the [001] direction (c axis) vertical. Fields up to 6.5 T were applied in this direction. The room-temperature lattice parameters for $\text{Fe}_{0.6}\text{Zn}_{0.4}\text{F}_2$ are 3.24 Å in the [001] direction and 4.71 Å in the [100] and [010] directions. The incident wave vector was $k_i = 2.67 \text{ \AA}^{-1}$ and all horizontal collimations were 10', giving a wave-vector resolution half-width at half maximum (HWHM) of 0.0009, 0.0028, and 0.026 reduced lattice units (r.l.u.) in the transverse, longitudinal, and vertical directions, respectively. Nearly all data were taken by scanning the wave vector Q trans-

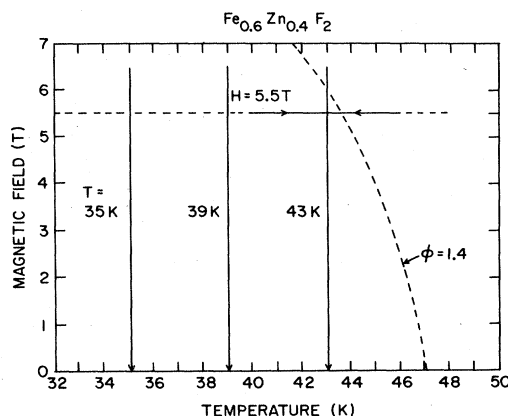


FIG. 1. Phase boundary in $\text{Fe}_{0.6}\text{Zn}_{0.4}\text{F}_2$ with several paths in H and T in the hysteresis study.

versely to Q_0 the (100) magnetic lattice point since the resolution is highest in such scans.

III. FIELD-COOLED BEHAVIOR

Initially experiments were performed with $H = 0$, and a well-defined transition to long-range antiferromagnetic order was observed at 47.1 K. The Bragg scattering from the long-range order had an approximately Gaussian profile with only very weak tails. The critical behavior at $H = 0$ is consistent with that studied in detail¹¹ in $\text{Fe}_{0.5}\text{Zn}_{0.5}\text{F}_2$, and is discussed further in Sec. V.

Experiments were then performed to study the field cooled, (FC) behavior in which the sample is warmed above $T_N(0)$, the field fixed and the sample cooled slowly through $T_N(H)$. Figure 1 illustrates this procedure and the phase-boundary line determined by birefringence measurements.⁸ Figure 2 shows the temperature dependence of the HWHM obtained from FC scans at 5.5 T; the other scans will be discussed later. The peak width decreases

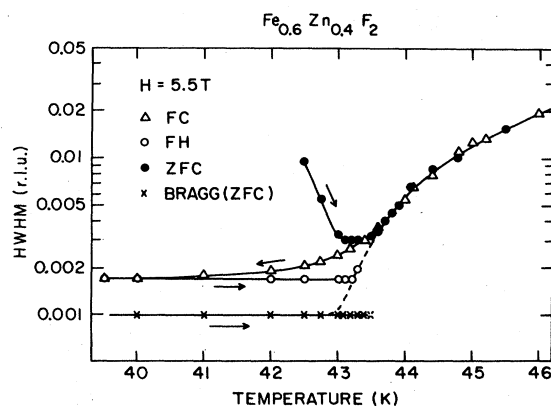


FIG. 2. HWHM vs T observed in the $(1, \xi, 0)$ transverse scans for the FC (cooling in a field H), FH (reheated after FC), and ZFC (cooling with $H = 0$, then applying H and heating) procedures with $H = 5.5 \text{ T}$. The dashed line is the ZFC HWHM when the Bragg and broader components are not separated.

smoothly with decreasing temperature and is temperature independent below ~ 40 K with a limiting value of 0.0017 ± 0.0001 reciprocal-lattice units (r.l.u.), significantly broader than the transverse resolution of 0.0009 r.l.u. The low-temperature limiting width decreases with decreasing applied field for each FC scan as expected. However, for fields less than about 3.0 T the limiting width is the resolution width, implying that the correlation length exceeds 300 lattice constants.

In Fig. 3 we show the peak intensity for $\mathbf{Q} - \mathbf{Q}_0 = \mathbf{q} = (0, 0, 0)$ as a function of applied field. The peak intensity initially increases with increasing field, reaches a plateau at about 4.0 T and then decreases for fields above 5.5 T. This behavior was seen previously in both the $\text{Co}_{0.35}\text{Zn}_{0.65}\text{F}_2$ and the $\text{Fe}_x\text{Zn}_{1-x}\text{F}_2$ samples and has been discussed in detail in Ref. 7. It arises because these crystals are crystallographically very perfect and so the intense magnetic Bragg reflection is strongly limited by extinction. When the magnetic order breaks up into domains, this extinction is reduced and the total scattered intensity increases. For fields above 4 T this increase in intensity with increasing field is compensated by the increasing width taking the scattered intensity out of the resolution function. Figure 3, therefore, provides evidence that fields as low as 1 T destroy the long-range order even though the length scale is much greater than the resolution function.

Experiments on $\text{Fe}_x\text{Zn}_{1-x}\text{F}_2$ with $z = 0.35$ and 0.5 have shown that the low-temperature FC profiles are accurately represented by

$$S(\mathbf{Q}) = \frac{CK}{(K^2 + q^2)^2} \quad (1)$$

with $\mathbf{q} = \mathbf{Q} - \mathbf{Q}_0$ and \mathbf{q} in reciprocal-lattice units. The low-temperature FC results of the $x = 0.6$ sample with $H = 5.5$ T were fitted to Eq. (1) and yield $K = 0.0012 \pm 0.0003$ r.l.u. corresponding to a correlation length of about 130 lattice constants.

The weak tails of the FC distributions are unaffected by the extinction. As is evident from Eq. (1), if C is a con-

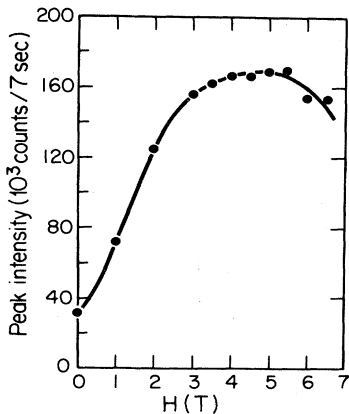


FIG. 3. Peak intensity as a function of magnetic field at $T = 10$ K after field cooling.

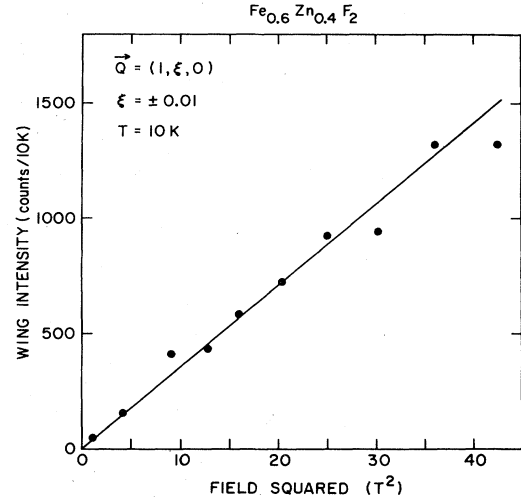


FIG. 4. Intensity for $\mathbf{Q} = (1, \pm 0.01, 0)$ vs H^2 for the FC sample at $T = 10$ K. The straight line suggests that $K \approx H^2$.

stant, and as demonstrated in previous experiments on $d = 3$ systems^{5,7} for $|q| \gg K$, the intensity at fixed q scales linearly with K . The intensity for $\mathbf{q} = (0, \pm 0.01, 0)$ as a function of H^2 is shown in Fig. 4, and shows that this intensity, and hence K , varies roughly linearly with H^2 . In $\text{Fe}_{0.35}\text{Zn}_{0.65}\text{F}_2$ and $\text{Fe}_{0.50}\text{Zn}_{0.50}\text{F}_2$ it was found⁷ that $K \approx H^{2.2 \pm 0.1}$. Thus the behavior in all three samples of $\text{Fe}_x\text{Zn}_{1-x}\text{F}_2$ is identical to within the errors. Using this H^2 scaling we may estimate that the domain sizes in $\text{Fe}_{0.6}\text{Zn}_{0.4}\text{F}_2$ at 1.41 T and 2.0 T are ~ 2000 and ~ 1000 lattice constants, respectively. It is clear therefore that the heat capacity at these fields could indeed exhibit quite sharp peaks since the domains contain, respectively, $\sim 1.6 \times 10^{10}$ and 2×10^9 spins.

In summary, the FC behavior in the $\text{Fe}_{0.60}\text{Zn}_{0.40}\text{F}_2$ crystal is closely similar to that observed previously in the more dilute samples.

IV. HISTORY-DEPENDENT BEHAVIOR

In order to compare with the birefringence results we first located the phase boundary using neutron techniques. In conventional neutron phase-transition studies, T_N may be accurately located by measuring the intensity as a function of temperature for a wave vector just off the Bragg peak; the intensity typically exhibits a sharp peak at T_N . FC scans do indeed exhibit peaks at about the expected temperatures; the peaks, however, become both more intense and very rounded with increasing applied field. A much sharper feature can be obtained using a different procedure. This involves cooling the sample with zero applied field into the Néel state, applying a field H and then heating the sample through $T_N(H)$. We refer to this as the zero-field-cooling (ZFC) procedure. Typical data obtained using the ZFC procedure are shown in Fig. 5. The peak intensity grows strongly with increasing field due to an increasing Lorentzian-squared contribution at the threshold temperature. We find that the ZFC wing peak temperature corresponds closely to that determined from

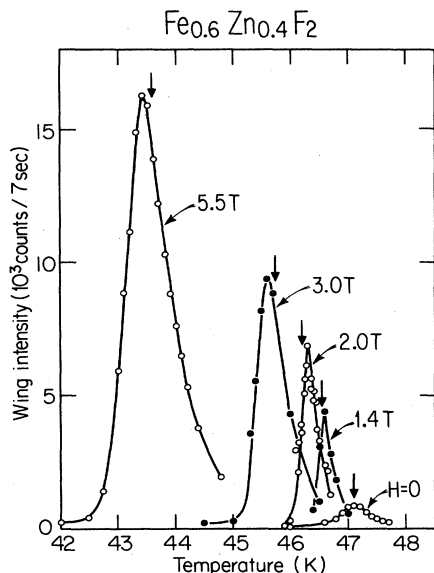


FIG. 5. Intensity for $Q=(1, \pm, 0.01, 0)$ vs T from ZFC scans at several fields. The arrows show the peak temperature of the heat capacity.

the peak in the heat capacity at all fields. The phase boundaries determined by birefringence and this neutron scattering technique are the same to within ≈ 0.2 K.

We now discuss the detailed history-dependent behavior. Data were taken using the ZFC procedure, the FC procedure and then reheating in the same field (FH).

The temperature dependences of the HWHM and the peak intensity are shown in Figs. 2 and 6, respectively, for each of these procedures in a field of 5.5 T. When the apparent HWHM and peak intensity of the ZFC line shapes

are plotted versus T , the width is resolution limited at low temperatures and smoothly increases above 42.75 K, whereas the peak intensity remains almost unchanged until 43.3 K, as is shown by dotted curves in Figs. 2 and 6. As seen in Fig. 7, however, the ZFC line shapes at temperatures just below the phase boundary are clearly separable into two components: a resolution-limited magnetic Bragg component and a much broader second component. The approximation HWHM and peak intensity of the separate Bragg and broader component are shown in the figures by crosses and solid circles, respectively. Far below the phase boundary, the ZFC system is in the extinction limited $H=0$ antiferromagnetic Néel state, as is indicated by the predominant resolution-limited Bragg peak. The secondary component is negligible. Upon raising the temperature, the intensity of the Bragg component decreases and vanishes near $T=43.5$ K, whereas the peak intensity of the broad component rapidly increases as this temperature is approached from below. The HWHM of the diffuse component decreases and shows a minimum near $T=43.25$ K. Since the concentration gradients give a smearing of $T_N \approx 0.4$ K the width of this minimum may result entirely from concentration gradients. As the temperature increases further, the HWHM increases while the peak intensity decreases.

Above the boundary, the data taken upon cooling the sample in a field (FC) are identical to the ZFC data. However, as we discussed in the preceding section, as the sample is cooled below the boundary in a field $H=5.5$ T, the HWHM remains larger than instrumental resolution and only gradually decreases, as shown in Fig. 2. Below $T \approx 40$ K the HWHM is constant at 0.0017 r.l.u. as the temperature is further reduced. The resolution-limited Bragg peak observed in the ZFC data does not occur. The peak intensity rises as the temperature decreases in a field of 5.5 T, and shows no sharp features near the phase

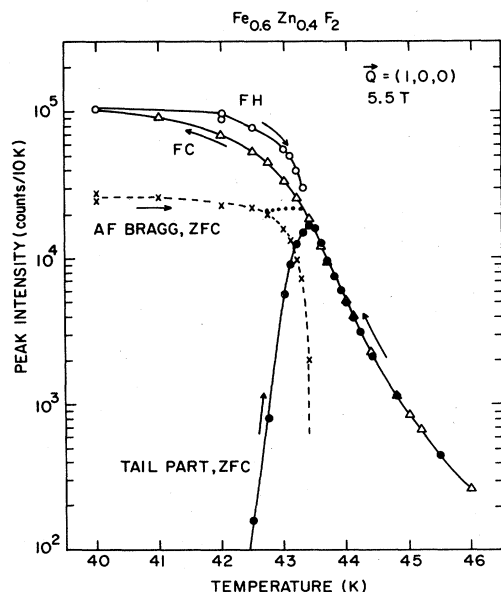


FIG. 6. Peak intensities vs T for the FC, FH, and ZFC procedures with $H=5.5$ T. The dotted line is the ZFC peak intensity if the Bragg and broader components are not first separated, and the dashed line the intensity of the Bragg peak.

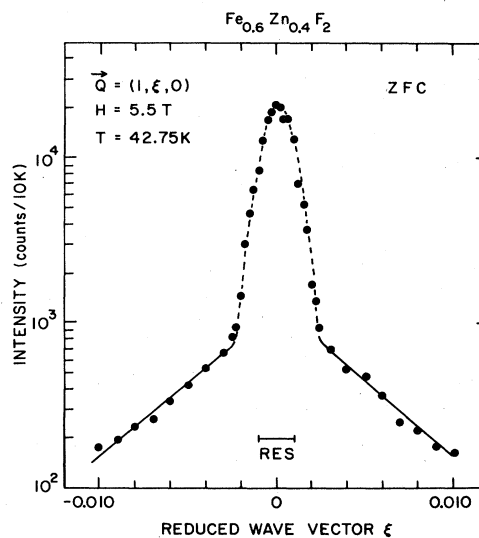


FIG. 7. Transverse ZFC scan below T_c demonstrating the Bragg and broader components.

boundary. The intensity is larger than in the zero-field measurements as a result of the extinction effect discussed in Sec. II.

After preparing the sample in the FC state at $T=40$ K, the temperature was increased (FH). The HWHM remained constant at the lowest value attained, 0.0017 r.l.u., until the phase boundary was approached, where it then merged with the curve of the apparent HWHM of the ZFC procedure. Relative to the FC case, the FH peak intensity was larger at all temperatures up to 43.4 K. We attribute this to the more ordered state relative to the FC case. Apparently, the increased size of the domain structure is not sufficient to increase significantly the extinction effect. For comparison, the line shapes of the scattering data observed at $T=43.0$ K and $H=5.5$ T are shown in Fig. 8 for the ZFC, FC, and FH states.

In order to characterize further these effects, we also studied the scattering as a function of the applied field along the paths indicated in Fig. 1. The sample was cooled in a field of 6.5 T to a temperature near the phase boundary. The field was then decreased to zero. Thus, in this configuration, the state is approached from the direction of more disorder as in the FC case. At 43 K, the boundary is crossed near 6 T and the HWHM is about twice the resolution, Fig. 9. As the field then decreases to $H=0$, the HWHM decreases to the resolution limit. For $T=39$ K, or 43 K, as the field is decreased, the HWHM at a given field agrees to within the errors with that obtained when the sample is field cooled to the same temperature in the same field H . These results show that at temperatures which are high enough that the system is able to relax, the identical state is achieved provided that

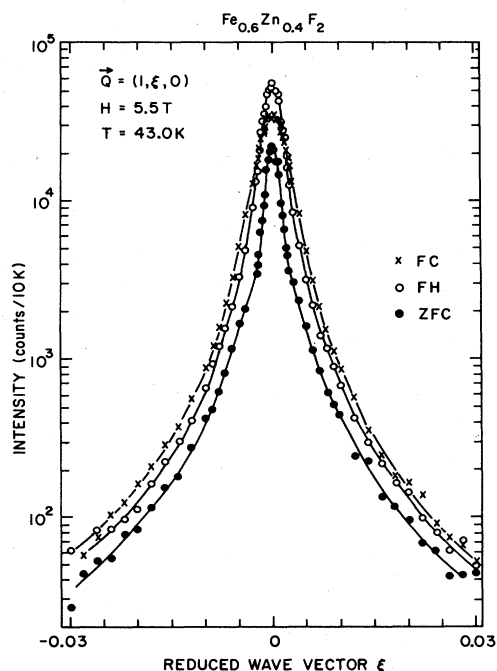


FIG. 8. Three scans at the same temperature below T_C showing the different intensities and small- ξ line shapes for FC, FH, and AFC procedures. The lines are guides to the eye.

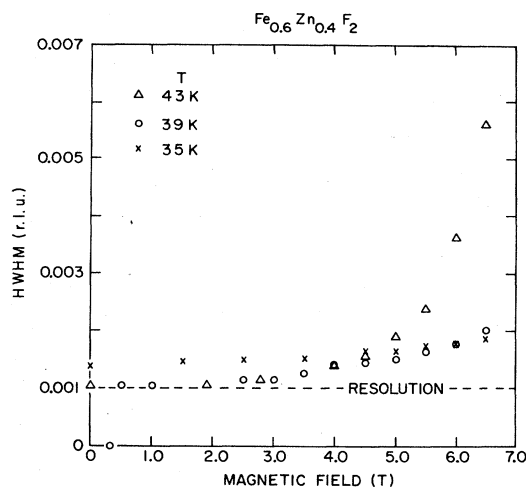


FIG. 9. HWHM as the field is reduced from 6.5 T along the three paths indicated in Fig. 1.

the state is approached from a more disordered direction, whether by field or temperature scans. At $T=35$ K, the HWHM does not decrease to the resolution limit as the field is reduced to zero, indicating the freezing to be expected in good Ising systems. At very low temperatures ($T < 10$ K) the HWHM is independent of changes in the field, indicating that the system is frozen and that the time required for relaxation to the long-range antiferromagnetic state as $H \rightarrow 0$ is extremely long.

In Fig. 10 the peak intensities are plotted versus the applied field when the field is reduced at 35, 39, and 43 K. For all temperatures the peak intensity initially increases, as expected, since the system is becoming more ordered. However, at smaller fields the extinction effect begins to

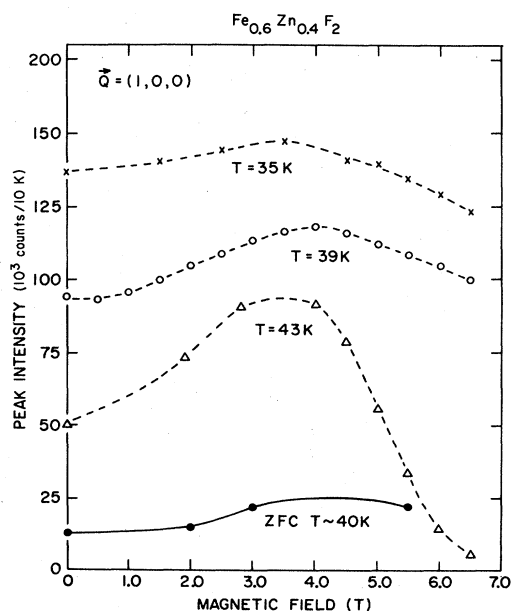


FIG. 10. Peak intensity vs H for the FC sample along the three paths indicated in Fig. 1 and for the ZFC procedure.

dominate, causing the intensity to decrease as the field is further reduced. The zero-field intensity is, however, still much larger than the peak intensity observed when the sample is cooled to these temperatures in zero field (ZFC). This larger intensity is attributable to a smaller extinction effect and therefore suggests that the system is in a less ordered state.

We studied the time dependence of the FC state at $T=25$ K in zero field, on rapidly reducing the field from 6.5 to 0 T. The line shape was measured every 10 min for several hours. Figure 11 shows the line shapes observed initially, 20 min later, and 8 h later. A small but measurable relaxation towards the more ordered state as judged by the intensity in the wings is evident. Thus the system at $T=25$ K in the absence of the random field continues to relax even 8 h later. We also studied the time dependence of the FC line shape 100 mK below the phase boundary with the magnetic field held constant at 3.0 T. In this case, the line shape measured after 6.5 h agreed well with the initial scan, except for a few points with $|\xi| < 0.001$, whose intensities increases by up to 4% in the first 1.5 h. Thus the disordered state obtained in the FC procedure is stable for all reasonable time scales even very close to the phase boundary.

Finally, we also carried out scans with the FC and ZFC procedures at a number of smaller fields. The behavior is similar to that discussed above for 5.5 T, the FC and ZFC procedures yield identical results above the phase boundary but the results are history dependent below the boundary. Thus the history-dependent effects are confined to the temperature region at and below the heat-capacity peak temperature for any given field, while for temperatures less than about $0.8T_N(0)$ the system is completely frozen. Above this latter temperature, for all fields at which the HWHM is measurably above the resolution width identical results are obtained if the state is approached from the more disordered direction, but dif-

ferent results are found when approached from the more ordered directions. This implies that in the state below $T_N(H)$, the domains are able to dilate to a reproducible diameter but cannot then contract.

V. CRITICAL BEHAVIOR

In the preceding section we have shown that the results obtained above the phase boundary are independent of the past history of the sample. It is, therefore, possible to study the behavior of the spin-spin correlation function above the phase boundary and in the same temperature regions probed by the birefringence study.

Critical scattering measurements were, therefore, performed with applied fields of 0, 1.4, 2.0, 3.0, 5.5, and 6.5 T; part of the 1.4- and 2.0-T data were taken by Belanger and Yoshizawa²⁰ using the masked configuration described in Sec. III and are also reported by Belanger *et al.*¹² Typical data are shown in Fig. 12 and the HWHM are shown in Fig. 13. It is evident that the temperature dependence of the HWHM and hence of the critical scattering is significantly different in an applied field from that in zero field.

In particular the temperature dependence of the HWHM for $H=0$ is clearly curved corresponding to an exponent $\nu < 1$, whereas in an applied field, the temperature dependence of the HWHM corresponds over a significant temperature region to a behavior which is closely linear with $T-T_0$. At the higher applied fields especially, the HWHM tends to curve above the linear lines when the HWHM is small.

The behavior of the width for $T=T_N(H=0)$ as a function of applied field is shown in Fig. 14. A preliminary analysis of the observed behavior gives the width

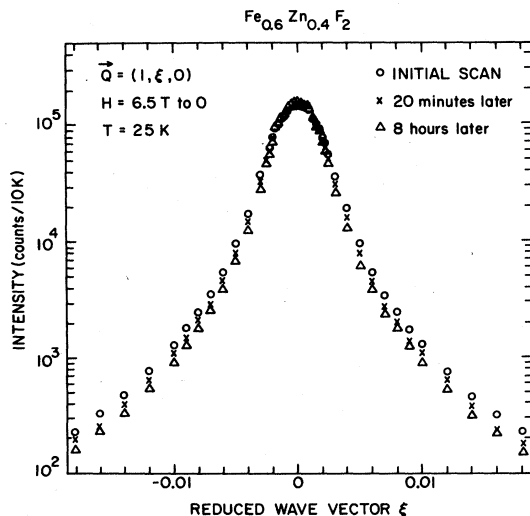


FIG. 11. The time dependence of the scattering when the field is rapidly reduced from 6.5 T to 0 T at 25 K.

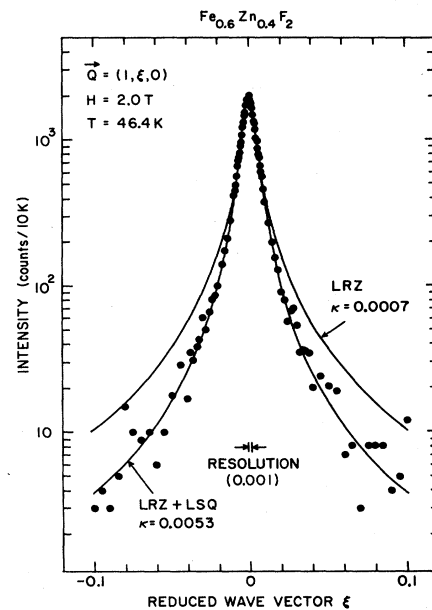


FIG. 12. Transverse scan with $H=2.0$ T. As the figure illustrates, Lorentzian line shape is inadequate to describe the data, whereas the Lorentzian plus a squared-Lorentzian form, Eq. (2), fits very well.

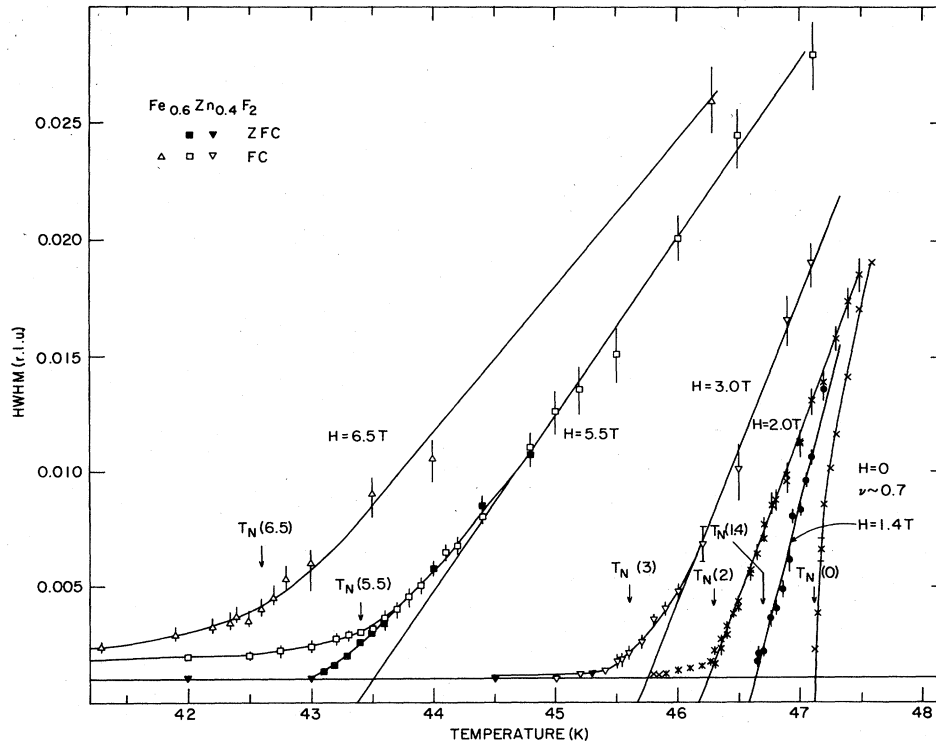


FIG. 13. Measured HWHM as a function of temperature for $H=0, 1.4, 2.0, 3.0, 5.5,$ and 6.5 T. The lines are guides to the eye or straight lines. At 3.0 and 5.5 T the filled points were obtained with the ZFC procedure and the open points with the FC procedure.

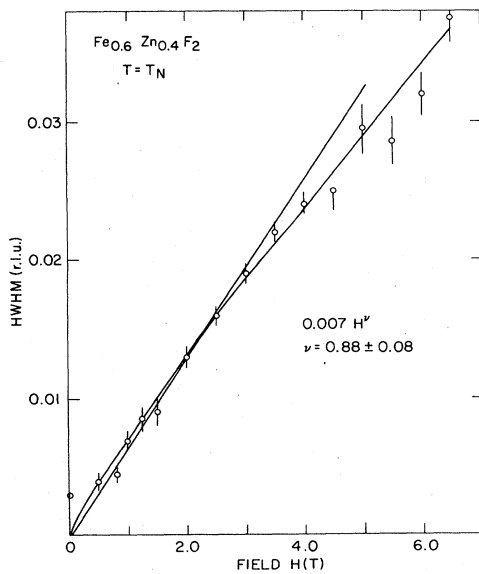


FIG. 14. The HWHM as a function of field for $T=T_N$. One solid line is a straight line corresponding to $\nu=1.0$ and the other to $\nu=0.88\pm 0.08$.

proportional to H^ν with $\nu=0.88\pm 0.08$. This may be compared with the theoretical prediction by Aharony and Pytte,¹³ $\nu=(1-\eta/2)^{-1}\approx 1.02$, and with the result obtained⁷ in $\text{Fe}_{0.35}\text{Zn}_{0.65}\text{F}_2$; namely, $\nu=0.86\pm 0.04$. Clearly there is excellent agreement with the earlier experimental results. The difference between the experimental results and the theoretical prediction may arise because of nonasymptotic terms in the experimental measurements.

Further analysis can only be performed once the form of $S(\mathbf{Q})$ is known. We have already shown^{5,7} that

$$S(\mathbf{Q}) = \frac{A}{K^2 + q^2} + \frac{B}{(K^2 + q^2)^2} \quad (2)$$

gives a good amount of the scattering at all temperatures in $d=3$ Ising systems. This form has also been obtained theoretically in the mean-field approximation by, for example, Mukamel and Pytte.¹⁵ In Eq. (2) the Lorentzian term arises from the susceptibility so that

$$k_B T \chi_s(\mathbf{q}) = \frac{A}{K^2 + q^2}, \quad (3)$$

while the Lorentzian-squared terms arises from the moments induced by the random fields.

The results were fitted to Eq. (2) convoluted with the experimental resolution function. In the case of $H=0$, only the Lorentzian term is applicable and the results are

consistent with the more comprehensive study¹¹ made of $\text{Fe}_{0.5}\text{Zn}_{0.5}\text{F}_2$; that is $K \approx \tau^\nu \approx (T/T_N - 1)^\nu$ with $\nu = 0.73$ and $A/K^2 \approx \tau^{-\gamma}$ with $\gamma = 1.44$. Typical fits of Eq. (2) to the data at $H = 2.0$ T, and $T = 46.4$ K are shown in Fig. 12. The Lorentzian fit with $B = 0$ is clearly unsatisfactory but when both terms are included the fit is excellent, and the Lorentzian term contributes 5% of the peak intensity. All of the data could be well described by Eq. (2) which, while it does not prove the uniqueness of the Lorentzian and Lorentzian-squared profile, does demonstrate that the form gives a good description of the results. The temperature dependence of the parameters K , A , and B from this preliminary analysis have been discussed in detail for $H = 1.4, 2.0$ T by Belanger *et al.*¹² Here we note only that A and B are both largely independent of temperature to within the errors while K varies linearly with $T - T_0$ with T_0 within 0.2 K of the ZFC critical scattering peak temperature determined as in Fig. 5.

VI. DISCUSSION AND CONCLUSIONS

The results of these experiments will be briefly summarized. Firstly, when the sample is cooled in a field (FC) long-range order is not established and the results are very similar to those obtained on the $d = 3$ systems; $\text{Co}_x\text{Zn}_{1-x}\text{F}_2$, $\text{Mn}_x\text{Zn}_{1-x}\text{F}_2$, and $\text{Fe}_x\text{Zn}_{1-x}\text{F}_2$ with x ranging from 0.26 to 0.75. The scattering profiles below the phase boundary are Lorentzian squared in form and $K \approx H^2$.

Secondly, the history dependences of the low-temperature state has been studied in detail. Below a well-defined temperature, which coincides within the errors with the heat-capacity peak value, the properties of the system depend on its prior history, whereas above this temperature they do not. Just below this temperature it is possible for the domains to relax in the direction of more order towards the FC state by further lowering the temperature or reducing the field, but not towards a more disordered state. At low temperature $T < 0.8T_N$, the system is frozen and no relaxation occurs. Immediately below T_N the disordered FC state is unchanged for times between minutes and six hours.

Thirdly, the critical phenomena above the history-dependent boundary has been measured; the results of K are consistent over a limited temperature interval with a linear variation of K vs $T - T_0$, although T_0 is not known precisely enough to determine an effective exponent accurately.

Many recent theories¹⁴ suggest that in equilibrium the lower critical dimension of the random-field problem, d_l , is 2. This result, however, is not obviously consistent with the FC neutron scattering results which do not achieve long-range order at low temperatures. These theories do not address the history dependence of the low-temperature state, discussed in Sec. III. This behavior may be understood qualitatively with the aid of the mean-field computer simulations of Yoshizawa and Belanger.¹⁶ When the system is cooled near the Néel temperature the clusters order in a direction determined by the local imbalance of the spins on the two sublattices. On further cooling these

clusters grow until local free-energy barriers produced by the random field effectively pin the domain walls so that the large domains can no longer reverse their orientation. The system cannot then establish long-range order even if this is the ground state.

Below the history-dependent boundary the barriers are too large to allow domain-wall motion, but if the applied field is reduced, these barriers are also reduced and the system is able to relax to a state of more order. When the field is increased, however, the local free-energy barriers prevent the nucleation of new domain walls and so new domains are not formed until the history dependent boundary is reached. As the boundary is approached the barrier pinning energy and thermal fluctuations become of comparable energy and allow domain-wall nucleation so that the system transforms to the high-temperature equilibrium state.

This picture is necessarily tentative being based on a mean-field-theory simulation, and so cannot give information about the crucial aspects of domain-wall dynamics and pinning. Fortunately, this aspect has been studied theoretically very recently. Villian¹⁷ and Grinstein and Fernandez¹⁸ have discussed the behavior of systems in a field quenched from the paramagnetic state to low temperatures. In both cases they find, for $d < 4$, that there will be large energy barriers to the motion of domain walls; they predict that after a time the domains will have expanded to a size

$$R_c = \frac{JT}{H_{\text{RF}}^2} \ln(t/\tau), \quad (4)$$

where τ is a microscopic time and H_{RF} is the strength of the random field. Equation (4) predicts $K \approx H^2$, which is in accord with our observations; substitution of the magnitude for J , H_{RF} , and $\tau = \hbar/J$ into Eq. (4) gives, for $H = 5.5$ T and $t = 100$ sec, $R_c = 400$ lattice constants, in reasonable accord with our observation of ≈ 130 lattice constants. The theory also naturally accounts for the fact that domains can expand to a metastable reproducible radius but not contract as discussed in Sec. III. We consider the above an important success for the dynamical theories and, to the extent that they are based on $d_l = 2$, this agreement maybe viewed as indirect support for 2 as the lower marginal dimensionality of the random-field Ising model.

It should be emphasized, however, that the dynamical theories, at present, study the motion of quenched domain walls in the lower temperature phase well below the phase boundary. Therefore these theories do not account for the abrupt transition between history-dependent behavior and history-independent behavior in the vicinity of the phase boundary; these models also fail to account for the extreme stability of the history-dependent states just below the phase boundary, as discussed in Sec. III.

The results obtained above the phase boundary may be viewed as consistent over a limited temperature range with two-dimensional Ising behavior as suggested first from birefringence measurements. Belanger *et al.*,¹² interpret this result as evidence for the $d_l = 2$ theories and a dimensionality shift of 1 for the $d = 3$ Ising model in a random field. However, because of the complicated behavior in the vicinity of the phase boundary, the con-

comitant uncertainty in T_0 and the strong correlations in the fits between the Lorentzian and Lorentzian-squared amplitudes, we are reluctant to draw any conclusions at all about the exponents in the paramagnetic phase.

It is clear that further theoretical and experimental work is needed to clarify the high-temperature behavior near the phase boundary. On the experimental side more experiments are needed to clarify the properties close to the phase boundary with still more uniform crystals to reduce the rounding from a lack of uniformity in concentration. On the theoretical side, a recent theory by Imbrie²¹ rigorously proves that the ground state at $T=0$ of the random-field Ising model in $d=3$ is the ferromagnetic state. However, these experiments as well as previous work by ourselves and others demonstrate that history-dependent effects dominate the physics of the three-dimensional random-field Ising model. Theory for the

time-dependent behavior in the immediate vicinity of the phase boundary is urgently required.

ACKNOWLEDGMENTS

We are grateful to G. Aeppli, A. Aharony, P. Bak, G. Grinstein, Y. Imry, Y. Shapira, and P. Wong for helpful discussions, D. P. Belanger for his contribution to this work, and M. Blume and V. Emery for support. The $\text{Fe}_{0.6}\text{Zn}_{0.4}\text{F}_2$ crystal was grown at University of California at Santa Barbara, Material Preparation Laboratory by N. Nighman. A. R. King and V. Jaccarino initially collaborated on this work. The work done at Brookhaven was supported by the Division of Materials Sciences U. S. Department of Energy under Contract No. DE-AC02-76CH00016 and that at Massachusetts Institute of Technology by the National Science Foundation, Low Temperature Physics, Grant No. DMR79-23203.

*Permanent address: Institute for Solid State Physics, University of Tokyo, Roppongi, Minato-ku, Tokyo 106, Japan.

†Permanent address: Department of Physics, University of Edinburgh, Mayfield Road, Edinburgh EH9 3JZ, UK.

¹Y. Imry and S. Ma, Phys. Rev. Lett. **35**, 1399 (1975).

²S. Fishman and Aharony, J. Phys. C **12**, L729 (1979).

³H. Rohrer, J. Appl. Phys. **52**, 1708 (1981).

⁴Y. Shapira, J. Appl. Phys. **53**, 1931 (1982); Y. Shapira and N. F. Oliveria, Jr., Phys. Rev. **B27**, 4336 (1983).

⁵H. Yoshizawa, R. A. Cowley, G. Shirane, R. J. Birgeneau, H. J. Guggenheim, and H. Ikeda, Phys. Rev. Lett. **48**, 438 (1982); M. Hagen, R. A. Cowley, S. K. Satija, H. Yoshizawa, G. Shirane, R. J. Birgeneau, and H. J. Guggenheim, Phys. Rev. B **28**, 2602 (1983); R. A. Cowley, J. Magn. Magn. Mater. **31-34**, 1439 (1983); R. J. Birgeneau, H. Yoshizawa, R. A. Cowley, G. Shirane, and H. Ikeda, Phys. Rev. B **28**, 1438 (1983).

⁶R. A. Cowley and W. J. L. Buyers, J. Phys. C **15**, L1209 (1982); R. A. Cowley, H. Yoshizawa, G. Shirane, M. Hagen, and R. J. Birgeneau, Phys. Rev. B **30**, 6650 (1984).

⁷For reviews of the neutron work see R. A. Cowley, R. J. Birgeneau, G. Shirane, and H. Yoshizawa, in *Multichannel Phenomena*, edited by R. Pynn (Plenum, New York, 1984), and R. J. Birgeneau, R. A. Cowley, G. Shirane, and H. Yoshizawa, J. State. Phys. **34**, 817 (1984). Experiments in $\text{Fe}_{0.5}\text{Zn}_{0.5}\text{F}_2$ and $\text{Fe}_{0.35}\text{Zn}_{0.65}\text{F}_2$ are presented in detail in R. A. Cowley, H. Yoshizawa, G. Shirane, and R. J. Birgeneau, Z. Phys. B **58**, 15 (1984).

⁸D. P. Belanger, A. R. King, and V. Jaccarino, J. Appl. Phys. **53**, 2702 (1982); Phys. Rev. Lett. **48**, 1050 (1982); D. P. Belanger, A. R. King, V. Jaccarino, and J. L. Cardy, Phys. Rev. B **28**, 2522 (1983).

⁹I. B. Ferreira, A. R. King, V. Jaccarino, and J. L. Cardy, Phys. Rev. B **28**, 5192 (1983).

¹⁰P. Z. Wong, S. VonMolnar, and P. Dimon, J. Appl. Phys. **53**, 7954 (1982); P. Wong and J. Cable, Phys. Rev. B **28**, 5361 (1983).

¹¹R. J. Birgeneau, R. A. Cowley, G. Shirane, H. Yoshizawa, D. P. Belanger, A. R. King, and V. Jaccarino, Phys. Rev. B **27**, 6747 (1983); **28**, 4028(E) (1983) and references therein.

¹²D. P. Belanger, A. R. King, and V. Jaccarino, preceding paper, Phys. Rev. B **31**, 4538 (1985).

¹³A. Aharony and E. Pytte, Phys. Rev. B **27**, 5872 (1983)

¹⁴J. F. Fernandez, G. Grinstein, Y. Imry, and S. Kirkpatrick, Phys. Rev. Lett. **51**, 203 (1983); G. Grinstein and S. Ma, *ibid.* **49**, 684 (1982); Phys. Rev. B **28**, 2588 (1983); Y. Shapira and A. Aharony, J. Phys. C **15**, 1391 (1982); J. Villian, J. Phys. (Paris) Lett. **43**, L551 (1982); K. Binder, Z. Phys. B **50**, 343 (1983).

¹⁵K. Binder, Y. Imry, and E. Pytte, Phys. Rev. B **24**, 6736 (1981); H. S. Kogon and D. J. Wallace, J. Phys. A **14**, L527 (1981); D. Mukamel and E. Pytte, Phys. Rev. B **25**, 4779 (1982); G. Parisi and N. Sourlas, Phys. Rev. Lett. **43**, 744 (1979); E. Pytte, Y. Imry, and D. Mukamel, *ibid.* **46**, 173 (1981); A. P. Young, J. Phys. C **10**, L257 (1977).

¹⁶H. Yoshizawa and D. P. Belanger, Phys. Rev. B **30** 5220 (1984).

¹⁷J. Villian, Phys. Rev. Lett. **52**, 1534 (1984).

¹⁸G. Grinstein and J. F. Fernandez, Phys. Rev. B **29**, 6389 (1984).

¹⁹R. Bruinsma and G. Aeppli, Phys. Rev. Lett. **52**, 1547 (1984).

²⁰D. P. Belanger and H. Yoshizawa (unpublished).

²¹J. Z. Imbrie, Phys. Rev. Lett. **53**, 1747 (1984); Commun. Math. Phys. (to be published).